A computationally effective dynamic hysteresis model taking into account skin effect in magnetic laminations

Olivier de La Barrière, Carlo Ragusa, Carlo Appino, Fausto Fiorillo, Martino Lobue, Frederic Mazaleyrat

A computationally effective dynamic hysteresis model taking into account skin effect in magnetic laminations

O. de la Barrière[1], C. Ragusa[2], C. Appino[3], F. Fiorillo[3], M. LoBue[1], F. Mazaleyrat[1]

[1] SATIE, ENS Cachan, CNRS, UniverSud, 61 av du Président Wilson, Cachan, France.
[2] Dip. Energia, Politecnico di Torino, C.so Duca degli Abruzzi 24, 10129 Torino, Italy.
[3] Instituto Nazionale di Ricerca Metrologica (INRIM), Torino, Italy.

Abstract

We propose a simplified dynamic hysteresis model for the prediction of magnetization behavior of electrical steel up to high frequencies, taking into account the skin effect. This model has the advantage of predicting the hysteresis loop and loss behavior versus frequency with the same accuracy provided by the Dynamic Preisach Model with a largely reduced computational burden. It is here compared to experimental results obtained in Fe-Si laminations under sinusoidal flux up to 2 kHz.

I. INTRODUCTION

The problem of high frequency behavior of magnetic laminations is of primary importance in modern electrical engineering problems [1], but difficult problems arise in the prediction and assessment of magnetization process and losses, because the skin effect compounds with the nonlinear hysteretic response of the material. In order to cope with the inhomogeneous profile of the flux density over the lamination thickness, the magnetic loss is generally calculated by numerically solving the diffusion equation over the sample cross-section, and using a dynamic hysteresis model for the material constitutive law [2]. The Dynamic Preisach Model (DPM) is the model of choice, because it is accurate and solidly established from the physical viewpoint [3][4]. Its application is, however, particularly time consuming, because calculations must be done for each finite element of the spatial mesh until convergence is reached. A faster approach, preserving the special virtues of DPM, would therefore be appropriate. We apply in this paper the DPM to the broadband behavior of nonoriented Fe-Si laminations through a simplified method, drastically reducing computing time and complexity of the full method, requiring the computation of the dynamics of each elementary hysteron distributed in the Preisach plane [5]. We start our discussion from the differential relation found by Bertotti [6] (formula (9), page 4609, of reference [6]) for the excess magnetic field due to the dynamic behavior of the magnetization process

$$H_{\mathrm{exc}}(t) \equiv H(t) - H_{\mathrm{stat}}(t) = \mathrm{sign}\left(\dot{H}_{\mathrm{stat}}\right)\frac{4}{3}\sqrt{\frac{\left|\dot{H}\right|}{k_{\mathrm{d}}}}, \tag{1}$$

where $H(t) = H_{\mathrm{a}}(t) - H_{\mathrm{cl}}(t)$ is the difference between the applied field $H_{\mathrm{a}}(t)$ and the counterfield $H_{\mathrm{cl}}(t)$ generated by the macroscopic eddy currents (classical field). $H_{\mathrm{stat}}(t)$ is the field that would provide under static conditions the same irreversible polarization J_{irr} and k_{d} [$\mathrm{A^{-1}s^{-1}m}$] is the DPM constant. Eq. (1) is derived under the simplifying assumptions of triangular $H_{\mathrm{a}}(t)$ and uniform Preisach distribution function. The extent to which such a restriction can be circumvented and the full DPM approach for generic exciting conditions and shape of the Preisach density function can be approximated will be discussed in the following. We find first that a numerical analysis based on (1) (Model 1) does not lead to highly accurate dynamic loop shapes, especially at high frequencies. A slight modification of (1) is therefore proposed (Model 2) and implemented in a non-linear magneto-dynamical model for the computation of the field distribution inside Fe-Si laminations, taking into account skin effect. The numerical results are compared with the experiments performed under sinusoidal flux up to 2 kHz.

II. THE SIMPLIFIED MODEL

A. The simplified DPM-Model 2

The Preisach distribution function, including the reversible contribution, was determined in a 0.35 mm thick Fe-(3.2wt%)Si-(0.5wt%)Al lamination, and the dynamic constant k_d=350 $A^{-1}s^{-1}m$ was identified. The full and the simplified (Model 1) DPM are compared in terms of the excess field. In this model benchmark, a sinusoidal dynamic field $H(t) = H_a(t) - H_{cl}(t)$ (peak value H_p = 100A·m^{-1}, frequency f = 200 Hz) has been applied. For the full DPM case, the excess field $H_{exc}(t) = H(t) - H_{stat}(t)$ is derived applying the DPM to $H(t)$ in order to get the irreversible polarization $J_{irr}(t)$, and then using the inverse static Preisach model to compute the static field $H_{stat}(t)$ from $J_{irr}(t)$. For the model 1, a numerical solution of (1) directly provides $H_{stat}(t)$ from the sinusoidal $H(t)$. A comparison between the results of two approaches is illustrated in Fig. 1 (the J_{irr} waveform obtained from the DPM has also been represented). Discrepancies are found between the two predicted $H_{exc}(t)$ waveforms, particularly around the reversal points of the irreversible magnetization J_{irr}. With the simplified Model 1 the zero of H_{exc} is, according to (1), coincident with the maximum of $H(t)$, whereas from the same picture, it appears that it occurs when J_{irr} is maximum. Consequently, (1) is formulated as

$$H_{exc}(t) \equiv H(t) - H_{stat}(t) = \mathrm{sign}\left(\dot{H}_{stat}\right)\frac{4}{3}\sqrt{\frac{\left|\dot{H}_{stat}\right|}{k_d}}\,, \tag{2}$$

on account of the fact that the sign of $\dot{H}_{stat}$ is the same as that of $\dot{J}_{irr}$. The simplified DPM based on

(2) (DPM-Model 2) appears now to provide (Fig. 1) an $H_{exc}(t)$ waveform in good agreement with the one provided by the full DPM.

Once the static field is known, $J_{irr}(H_{stat})$ is computed by means of the Static Preisach Model, while the reversible component $J_{rev}(H)$ is calculated ignoring any dynamic effect linked to the reversible contribution [1]. This procedure, which permits to obtain the constitutive law of the material $J(H)$, is summed up in Fig. 2. An example of hysteresis loop prediction (in this case with nested minor loop) is illustrated in Fig. 3, confirming the good agreement between the results provided by the full DPM and the simplified DPM-Model 2.

A. Numerical implementation of DPM-Model 2

This model requires solving the non-linear differential equation (2) for H_{stat} knowing the field H. This can be done putting (2) under an equivalent canonical form and adding the periodicity conditions (period T=1/f):

$$\begin{cases} \dot{H}_{\text{stat}} = \operatorname{sign}\left(H(t) - H_{\text{stat}}(t)\right) \cdot \dfrac{9k_{\text{d}}}{16} \cdot \left(H(t) - H_{\text{stat}}(t)\right)^2 \\ H_{\text{stat}}(0) = H_{\text{stat}}(T) \end{cases} . \tag{3}$$

and numerically solving it using a Runge-Kutta method. The application of this newly defined dynamical model to the computation of flux distribution inside the steel lamination can dramatically reduce the computational burden, as demonstrated in the next section.

III. MAGNETO DYNAMICAL MODELING AND EXPERIMENTAL

A. Magneto-dynamical model of the lamination

The solution of the diffusion equation over the lamination thickness with a dynamic hysteretic constitutive law requires a special numerical treatment of the non-linearity using the Fixed Point method [3][7]. The method proposed in [3] has been here implemented. The diffusion problem on the lamination thickness is one-dimensional, with the spatial coordinate x ranging over the lamination cross-section [-*e*/2; *e*/2] (where e = 0.35 mm is the lamination thickness). To solve the diffusion equation, the non-linearity of the material constitutive law *J(H)* is contained in a spatio-temporal function *R(x,t)*, called the residual [3] and the relationship between *H* and *J* is written as

$$H(x,t) = \upsilon_{\mathrm{FP}} \cdot B(x,t) + R(x,t)\,, \tag{4}$$

where υ_{FP} is a properly chosen constant, ensuring convergence [1]. Using (4), the diffusion equation can be written, with imposed mean flux density $B_{\mathrm{MEAN}}(t)$, in terms of vector potential *A* on a half lamination [0; *e*/2]:

$$\begin{cases} \upsilon_{\mathrm{FP}} \cdot \dfrac{\partial^2 A}{\partial x^2} - \sigma \dfrac{\partial A}{\partial t} = \dfrac{\partial R}{\partial x} \\ A(0,t) = 0 \ \text{ and } \ A(e/2,t) = -B_{\mathrm{MEAN}}(t) \cdot e/2 \\ A(x,t) \ \text{ is } T\text{-periodic} \end{cases} . \tag{5}$$

The time derivative and the time periodic condition are dealt with using temporal Fourier series [3]. More precisely, the residual function *R(x,t)* is decomposed into complex Fourier series for what concerns the time dependence. Equation (5) is then solved for each time harmonic, the time derivative becoming an algebraic multiplication by the corresponding harmonic pulsation. An inverse Fourier transformation permits to retrieve the function *A(x,t)*. For each time harmonic, the spatial second order derivative and the boundary conditions are dealt with using a numerical finite difference scheme (the half lamination is subdivided into 50 intervals). At the beginning of the iterative procedure, the residual *R* is initialized to zero and at each iteration step (index number *i*), the following process is performed:

1. Knowing the residual at the previous stage $R^{(i-1)}(x,t)$, the differential equation (5) is solved to compute the vector potential $A^{(i)}(x,t)$. The magnetic field is obtained as $H^{(i)}(x,t) = -\upsilon_{\mathrm{FP}} \dfrac{\partial A^{(i)}}{\partial x} + R^{(i-1)}(x,t)$.
2. A dynamic hysteresis model, providing the dynamic constitutive law *J(H)*, is used to evaluate $J^{(i)}$

from $H^{(i)}$ and the new induction value $B^{(i)}(x,t)=J^{(i)}(x,t)+\mu_0 \cdot H^{(i)}(x,t)$ is calculated. In [3], the dynamic hysteresis model is the DPM, and is replaced in this paper by the simplified model proposed in Fig. 2.

3. The new residual is then computed by $R^{(i)}(x,t)=H^{(i)}(x,t)-\upsilon_{\mathrm{FP}} \cdot B^{(i)}(x,t)$. The process is repeated until convergence of the residuals is obtained.

B. Results

The dynamic hysteretic constitutive law $J(H)$ of the material, which was in [3] given by the full DPM, has been here replaced by the model proposed in Fig. 2 where the Model 2 of the local excess field is applied. The Preisach distribution function has been identified following the method proposed in [1], in the previous 0.35 mm thick Fe-(3.2wt%)Si-(0.5wt%)Al lamination (conductivity σ = $1.773 \cdot 10^6$ S·m^{-1}, k_d=350 A^{-1}s^{-1}m). The magnetic loss and hysteresis loops have been measured under sinusoidal flux at different frequencies and peak inductions up to 2 kHz. The magnetic flux distribution and loss have been computed by applying the dynamical model, using both the full and the simplified DPM (Model 2). Fig. 4 provides an example of computed and experimental loops (J_p = 0.5 T, frequency f = 1 kHz). In Fig. 5 the comparison is made for energy loss versus frequency behavior. It shows the good predicting capability of the simplified dynamic Model 2, in spite of a computing time reduced by a factor around 60 with respect to the full DPM. Fig. 5 also shows the predicted loss behavior if the skin effect is ignored. In this case the induction is assumed uniform across the sample thickness and equal to the mean flux density $B_{\mathrm{MEAN}}(t)$. The classical loss is thus calculated according to

$$W_{\mathrm{class}} = \frac{\sigma e^2}{12} \int_0^T \left(\frac{dB_{\mathrm{MEAN}}}{\mathrm{d}t} \right)^2 \mathrm{d}t \tag{6}$$

It is found that ignoring the skin effect brings about a large overestimation of the loss above about f = 400 Hz, for the considered $B_{\mathrm{MEAN}}(t)$ peak value of 0.5 T considered in Fig. 5. An example of calculated induction profile $B(x, t_o)$ across the lamination thickness at a given instant of time t_o is shown in Fig. 6.

It refers to f = 1 kHz and a time t_o corresponding to the average flux density $B_{MEAN}(t_o) = 0$. Again, the full and simplified DPMs predict very close results.

IV. Conclusions

In this work we have discussed a novel dynamic model for energy losses and hysteresis loops in soft magnetic laminations based on simplified treatment of the Dynamic Preisach Model (DPM). It is applied on experiments performed up to the kHz range in Fe-Si sheets, in the presence of substantial skin effect, showing good agreement both with the experimental results and the prediction made using the full machinery of the DPM. A remarkable advantage in computing time, which is reduced by a factor around 60, is obtained substituting the full DPM with the present model.

References

[1] L.R. Dupre, O. Bottauscio, M. Chiampi, M. Repetto, and J. Melkebeek, *IEEE Trans. Magn.*, vol. 35, no. 5, pp. 4171-4184, 1999.
[2] S.E. Zirka, Y.I. Moroz, P. Marketos, and A.J. Moses, *Physica B: Condensed Matter*, vol. 343, no. 1, pp. 90-95, 2004.
[3] O. Bottauscio, M. Chiampi, C. Ragusa, M. Repetto, in "Studies in Applied Electromagnetics and Mechanics. Non-linear electromagnetic systems" (IOS Press, V. Kose and J. Sievert Editors, 1998) pp.449-454.
[4] O. Bottauscio, M. Chiampi, C. Ragusa, *J. Magn. Magn. Mater.* vol. 290-291, pp. 1446-1449, 2005.
[5] V. Basso, G. Bertotti, O. Bottauscio, M. Chiampi, F. Fiorillo, M. Pasquale, and M. Repetto, *J. Appl. Phys.* vol. 81 pp. 5606 – 5608, 1997.
[6] G. Bertotti, *Journal of applied physics*, vol. 69, no. 8, pp. 4608-4610, 1991**.**
[7] E. Dlala, A. Belahcen, and A. Arkkio, *IEEE Transactions on Magnetics*, vol. 43, no. 11, pp. 3969-3975, 2007.

Figure captions

Fig. 1- Excess fields provided by the full DPM, Model 1, and Model 2, for a sinusoidal dynamic field $H(t) = H_a(t) – H_{cl}(t)$ (frequency f = 200 Hz, field peak value H_p = 100A·m^{-1}) and corresponding irreversible polarization J_{irr} provided by the DPM in a 0.35 mm thick Fe-(3.2wt%)Si-(0.5wt%)Al lamination (dynamic constant k_d=350 A^{-1}s^{-1}m).

Fig. 2 - Block diagram of the simplified constitutive law *J(H)* of the material, using the Model 2 as a link between the field H and the static field H_{stat} (computation of the local excess field).

Fig. 3 - Example of the reconstructed $J(H)$ hysteresis loop with nested minor loops (f = 200 Hz, H_p = 150A·m^{-1})

Fig. 4 – Experimental and theoretical hysteresis loops at f = 200 Hz in the 0.35 mm thick Fe-(3.2wt%)Si-(0.5wt%)Al lamination for sinusoidal induction (B_p=0.5 T). The measurements have been performed on Epstein strips. Closed results are obtained by the full and the simplified DPM.

Fig. 5 – Same as Fig. 4 for the energy loss versus magnetizing frequency (DC – 2 kHz).

Fig. 6: Instantaneous induction profile $B(x,t_o)$ across the lamination thickness as obtained by the full and the simplified (Model 2) DPM (f = 1 kHz, -0.175 mm ≤ x ≤ 0.175 mm). The time t_o considered in this figure is the one for which the mean flux density $B_{MEAN}(t_o)$ = 0.

Figures

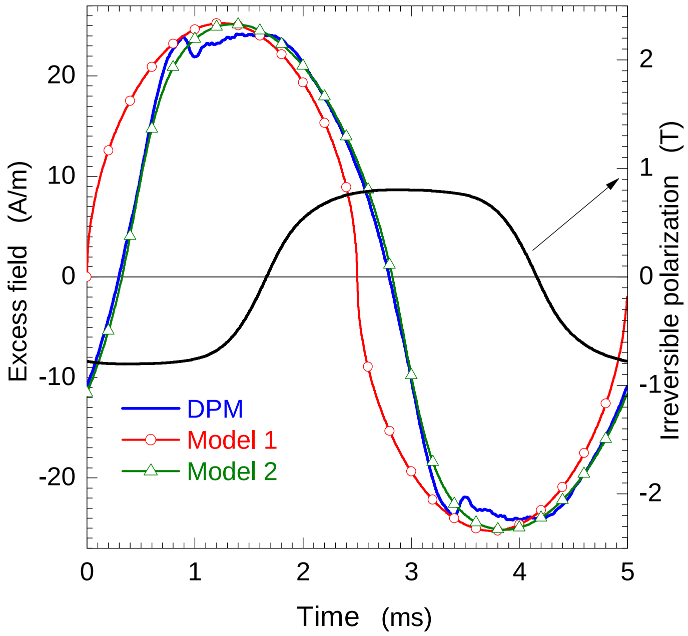

Fig. 1

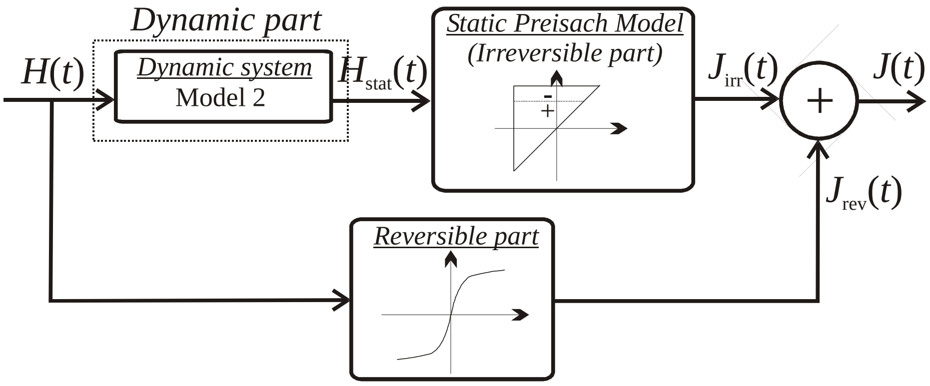
Dynamic part
H(t)
Dynamic system
Model 2
H_stat(t)
Static Preisach Model
(Irreversible part)
-
+
J_irr(t)
+
J(t)
J_rev(t)
Reversible part

Fig. 2

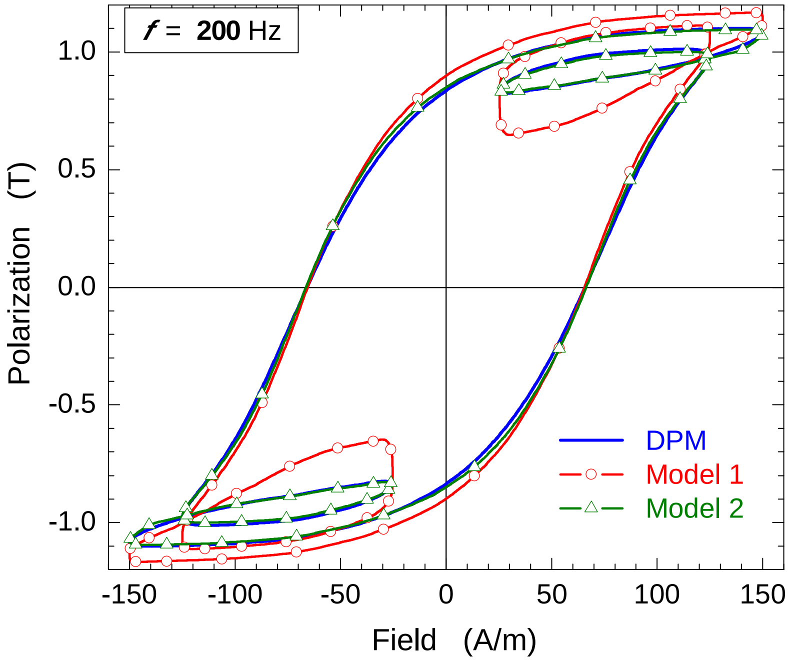
f = 200 Hz
Polarization (T)
1.0
0.5
0.0
-0.5
-1.0
-150
-100
-50
0
50
100
150
Field (A/m)
DPM
Model 1
Model 2

Fig. 3

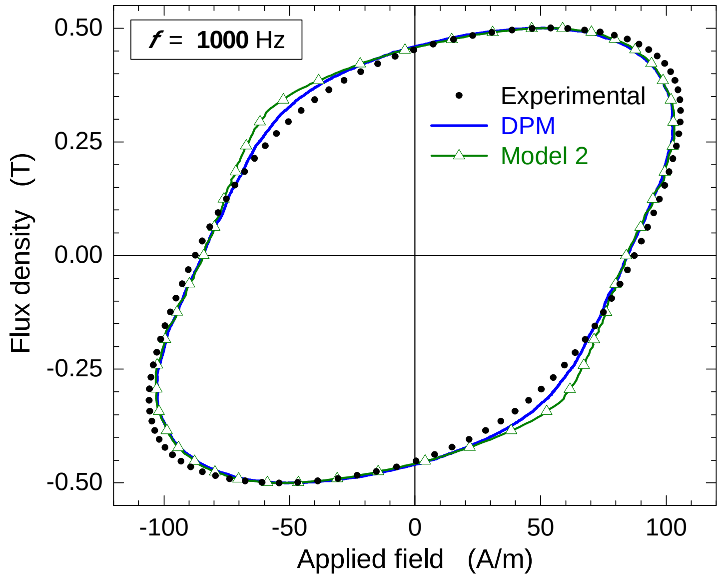
f = 1000 Hz
Experimental
DPM
Model 2
Flux density (T)
0.50
0.25
0.00
-0.25
-0.50
-100
-50
0
50
100
Applied field (A/m)

Fig. 4

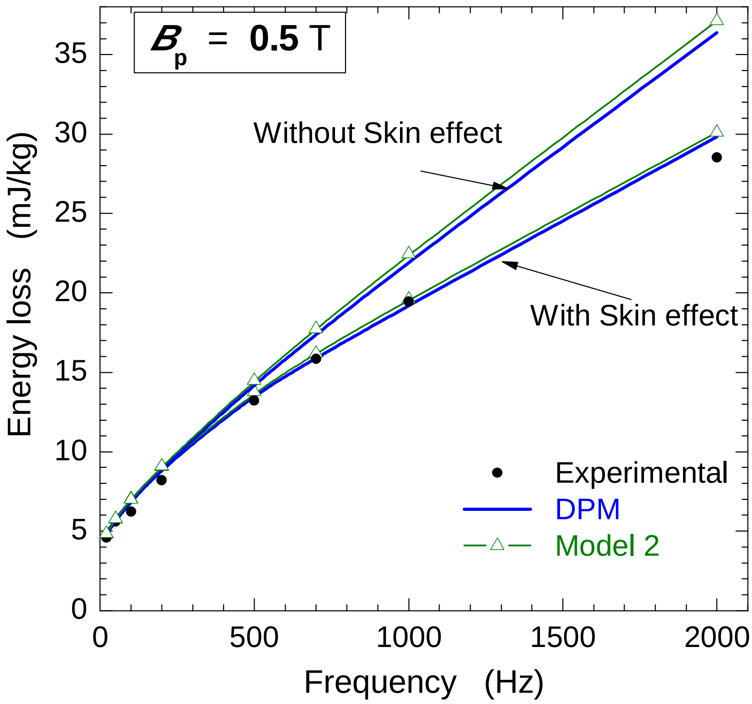
B_p = 0.5 T
Without Skin effect
With Skin effect
Experimental
DPM
Model 2
Energy loss (mJ/kg)
Frequency (Hz)
0
5
10
15
20
25
30
35
0
500
1000
1500
2000

Fig. 5

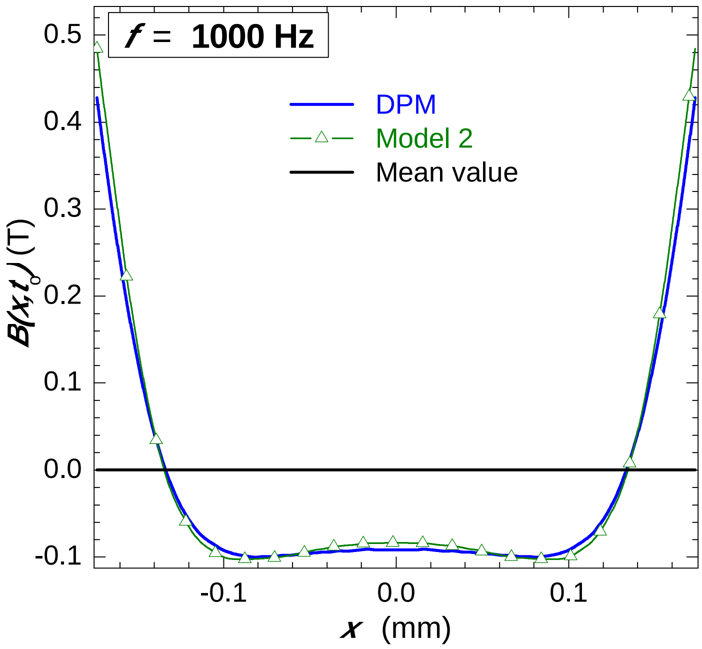
f = 1000 Hz
DPM
Model 2
Mean value
B(x,t0) (T)
x (mm)
0.5
0.4
0.3
0.2
0.1
0.0
-0.1
-0.1
0.0
0.1

Fig. 6